Experimental Study of a Combined Solar Heating and Radiative Cooling Device with an Adaptive Cover

Ariadna Carrobé, Marc Medrano, Cristian Solé, Ingrid Martorell, Lidia Rincón, Albert Castell

Sustainable Energy, Machinery and Buildings (SEMB) Research Group, INSPIRES Research Centre, Universitat de Lleida, Pere de Cabrera s/n, 25001 Lleida (Spain)

Abstract

Nowadays, climate change impact is becoming more important in our daylife and the use of renewable energy sources to cover the space conditioning and Domestic Hot Water (DHW) demands is growing every year. In this study, a new device that works with renewable energies and combines two different concepts, radiative cooling and thermal solar collection, is presented. The device is called Radiative Collector and Emitter (RCE) and it consists of a modified solar collector based on an adaptive cover. The absorber is covered by a polyethylene film and the glass of the solar collector is removed during the night to allow the radiative cooling effect. Due to this adaptive cover, during daytime the greenhouse effect is allowed because of the glass cover, favoring the solar collection; and during nighttime, radiative cooling is allowed through the polyethylene film in the same device. The adaptive cover allows the different properties of the materials to be used according to its mode of operation. This equipment has been experimentally tested during summertime 2019, in the University of Lleida, where the climate corresponds to a Semi-Arid Climate (BSk according to Köppen and Geiger climate classification). Results show that the RCE performs similarly to a solar collector during the day, with average heating values of 573.69 W/m^2, and is able to provide extra cooling at night, at an average cooling rate of 15.57 W/m^2.

Keywords: radiative cooling, solar thermal collection, renewable energy, adaptive cover, experimental setup

1. Introduction

The effects of climate change are becoming more dangerous and destructive day after day. The building stock is responsible for 40% of our energy consumption and 36% of all CO_2 emissions in the EU (European Commission, n.d.). Special efforts are being made in renovating the current building stock by energy efficiency means as well as considering the deployment of renewables (*UE 2018/844*, 2018). The use of renewable energy sources to cover space conditioning and DHW demands seems more likely over the years. While solar thermal energy can cover building heating and DHW demands (Kristin et al., 2016), there is not a technology with such potential and development for space cooling yet.

Alternatively, radiative cooling is a renewable cooling technology that uses the sky as a heat sink, benefiting from its effective temperature, which is much lower than ambient temperature. Energy can be dissipated to the sky taking advantage of the infrared atmospheric window (7–14 μm). This window allows infrared radiation to pass directly to outer space without intermediate absorption and re-emission in the atmosphere (Vall et al., 2020). The research for cover materials that allow this heat exchange to the atmosphere is focused on polymers, and the most common material tested and analyzed is polyethylene.

Most of the initial research conducted in this topic is related with the use of this technology, radiative cooling, during nighttime, because during daytime the power of solar radiation is higher than the net power of radiative cooling. However, recently some authors (Bhatia et al., 2018; Feng et al., 2019; Nilsson and Niklasson, 1995; Pech-May and Retsch, 2020; Yalçın et al., 2020) also studied the potential of radiative cooling during daytime. Some authors suggest that when combining the daytime solar heat collection and the nighttime radiative cooling, an extra overall power can be achieved with this combined system (Vall et al., 2020).

The main objective of this study is to analyze experimentally the combination of solar collection and radiative

© 2020. The Authors. Published by International Solar Energy Society
Selection and/or peer review under responsibility of Scientific Committee
doi:10.18086/eurosun.2020.06.03 Available at http://proceedings.ises.org

cooling in the same equipment. This equipment is called Radiative Collector and Emitter (RCE) and it relies on an adaptive cover using different optical properties for each functionality. This is, when the RCE works as a solar collector a high spectral transmittance in the solar radiation band and a very low spectral transmittance in the infrared band is required. On the other hand, during radiative cooling mode high spectral transmittance values in the atmospheric window wavelengths are required.

2. Experimental setup

The experimental setup consisted of a Radiative Collector and Emitter (RCE), two water tanks (the hot water tank has a heating coil), a heat exchanger, instrumentation and the control and data acquisition systems.

A sketch of the experimental setup is presented in Figure 1:

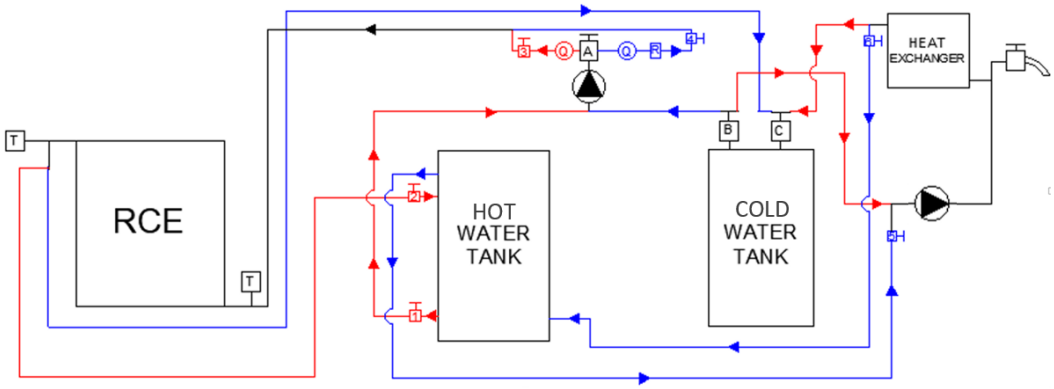

Figure 1: Sketch of the experimental setup. In red is colored the solar collection mode and in blue the radiative cooling mode.

Figure 1 presents the water flow coloured according to the mode and the direction of the flow. During solar collection mode (daytime, in red colour) water leaves the heating coil from the hot water tank (150 L) and passes through the pump and the Badger Meter flow meter. Directly water goes to the RCE device where temperature increases due to solar radiation and goes back to the heating coil to heat up the hot water tank. Meanwhile the water from the cold water tank (50 L), which has been cooled during nighttime, enters the water-air heat exchanger to increase its temperature until it reaches the exterior temperature, simulating a cooling demand.

During radiative cooling mode (night-time, blue) water leaves the cold water tank and passes through the pump and the Schmidt Mess flow meter entering the RCE to decrease its temperature due to radiative cooling. From the RCE it goes back to the cold water tank decreasing the temperature of the water in this tank. Meanwhile the water from the hot water tank, which has been heated during daytime, passes through the water-air heat exchanger decreasing its temperature to the exterior temperature, simulating a DHW demand.

To develop the RCE, a solar collector model BAXI SOL200, 2 m x 1 m x 80 mm, was modified. In this solar collector, the glass screen has been removed and the surface of the radiator has been painted with black paint in order to reduce the IR reflection of the absorber, as it is shown in Figure 2. These thermal images were taken with a thermal camera FLIR E6.

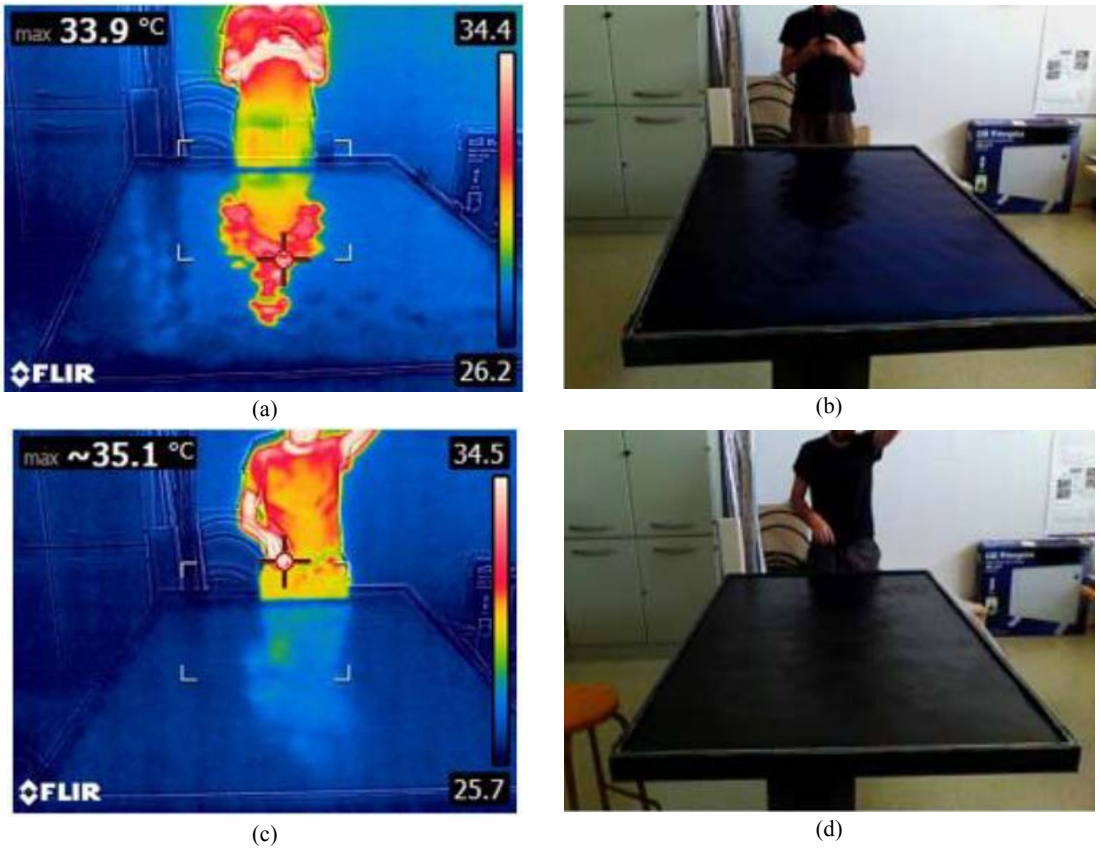

Figure 2: Above, there are the thermal camera (a) and the real (b) pictures of the normal absorber with selective surface, below there are the same pictures (c-d), taken with the absorber surface painted in black.

As Figure 2 shows, the absorber reduced the IR reflection after painting the surface with black paint. On the right pictures it is observed the color difference of the absorber: in (b) the absorber is dark blue whilst in (d), the absorber is completely black. The effect of having or not a selective surface in the absorber is observed on the left pictures where in (a) the IR reflection of the person is perfectly recorded by the thermal camera, whilst in (c) the reflection is almost non-existent.

To cover the absorber, the glass surface has been replaced by a 0.5 mm thick polyethylene film. To maintain the polyethylene film straight and prevent the film from bending, nylon ropes have been added every 15 cm in both directions of the collector, the long margin and the small one, as presented in the following Figure 3. This action was taken based on our experience with a previous prototype (Vall et al., 2020).

Figure 3: Nylon mesh located on the absorber in order to maintain straight the polyethylene film.

The transparent glass cover taken from the original solar collector is surrounded by an aluminium frame and four small wheels (Ø 15 cm, plastic 3D printed) are located in the shorter sides of the frame, two per each side. In the absorber, two long aluminium guides are attached in the shorter side. These guides are for the transparent glass to slide along them depending on the function mode. During day-time, the RCE is in solar collection mode, so the glass cover will be placed on top of the RCE; during night-time the glass cover will be removed and slid to the side. Thus the RCE will only have the polyethylene film as a cover for the radiative cooling.

Figure 4: RCE device with the glass cover sliding over the aluminium guides.

The experimental station is located in Lleida, where the climate is considered Semi-Arid (BSk) according to Köppen and Geiger classification and the data recorded are:

- The solar radiation, measured using a solar meter, model SMART SMP6 (2.5% accuracy).
- The external air temperature and relative humidity, using an Elektronik EE210 sensor (± 0.1 % uncertainty).
- The incoming infrared radiation with a pyrgeometer, model LP PIRG 01-DeltaOhm (5% accuracy).

In addition, the RCE device and the installation itself was monitored with the following equipment:

- The inlet and outlet temperatures of the water in the RCE were measured with platinum resistance thermometer Pt100 type 1/10 B DIIN. Accuracy at 20 °C: ±0.04°C.
- The water flow rate depends on the operating mode, so two flow meters were installed because the flow rates are very different between modes. To reduce the flow rate a restrictor valve is installed in the night mode circuit. For solar collection mode a Badger Meter-Primo Advanced (0.25% accuracy) is used whereas during the radiative cooling mode a Schmidt Mess-SDNC 503 GA-20 (4% accuracy) monitored the night flow.
- The acquisition data equipment consisted of a data logger model DIN DL-01-CPU, connected to the adapter data logger-computer model AC-250. The computer software to compile the data was STEP TCS-01. All data were registered and recorded at a time-frequency resolution of 1 min.

3. Methodology

The experimentation was performed during 6 weeks in summer 2019 in the University of Lleida (Spain). It was annotated daily in a field notebook the visual weather and sky conditions.

The results were analyzed weekly, corresponding to the following dates:

- 1st week: from 11th to 14th July, 2019
- 2nd week: from 15th to 21st July, 2019
- 3rd week: from 22nd to 28th July, 2019
- 4th week: from 29th July to 4th August, 2019
- 5th week from 5th to 11th August, 2019
- 6th week: from 12th to 16th August, 2019

It is important to highlight that data corresponding to the first week of analysis were only used to adjust the operation of the experimental facility and confirm that all the equipment was working properly.

According to the operational mode the flow range is set up as 0.8 L/min for radiative cooling mode and 1.8 L/min for solar collection mode.

Since the glass had to be slid manually and also the configuration of the valves to drive the fluid throughout the experimental set up was manual, a schedule for changing the modes was defined. Between 8 and 9 AM, the RCE would be set to the solar collection mode and the glass will be on top of the absorber; and between 8 – 9 PM, the RCE would start operation in the radiative cooling mode, so the glass will be slid aside to allow the refrigeration of the fluid. Transition modes of 2 h, between 7:30-9:30 AM and 7:30-9:30 PM were considered and experimental data for these periods were neglected to avoid transient unstable data. Thus, every day is defined as 10 h of solar collection mode (9:30 AM - 7:30 PM) and 10 h of radiative cooling mode (9:30 PM - 7:30 AM).

Mean values were calculated every 30 minutes for all the monitored parameters in order to analyze the behavior of the prototype.

Based on the measured solar radiation and IR sky radiation, days and nights were classified as clear or cloudy. This classification is based on a solar radiation and IR sky radiation ratio calculated respect to its maximum, taking 1000 W/m^2 for the solar radiation and 494 W/m^2 for the IR sky radiation.

The average power produced by the RCE, both during the solar collection mode and the radiative cooling mode, is calculated following this equation:

$$Power = \rho * C_p * \nu * \Delta T_{RCE} \quad \text{(eq. 1)}$$

Where:

ρ: Fluid density [km/m^3]

C_p: Specific heat of the fluid [KJ/kg·K]

ν: Volumetric flow taken from the flow meter located in the installation [m^3/s].

ΔT_{RCE}: Temperature difference of the fluid between the inlet and outlet point of the RCE [K].

4. Results and discussion

According to the previous section classification, in the following Figure 4, it is presented the daily average solar radiation ratio and IR radiation ratio, which were obtained dividing the daily average radiation considered (solar or IR) by the maximum radiations mentioned above.

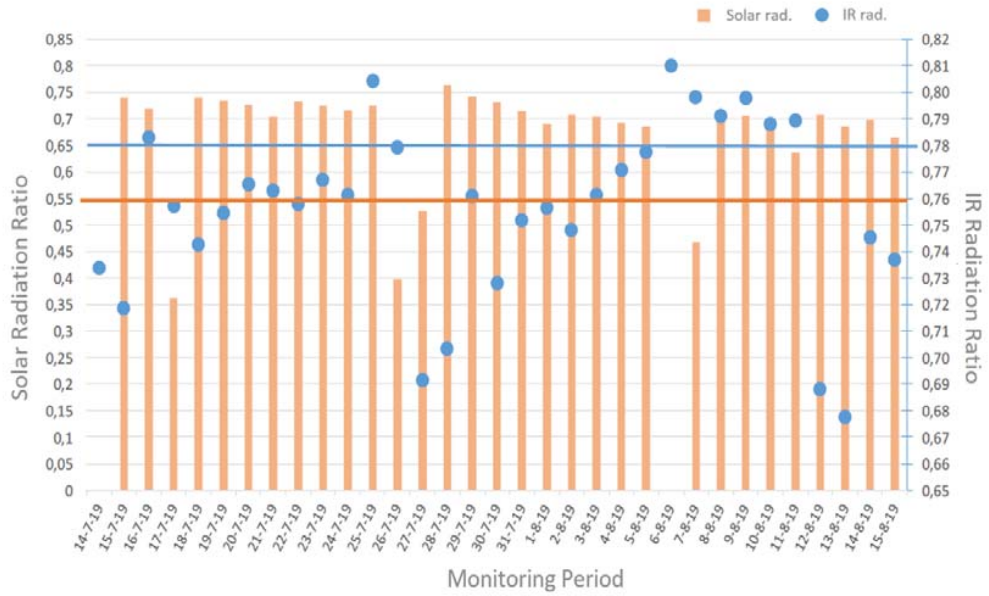

Figure 5: Average solar and IR radiation ratio in daily basis. In orange the solar radiation ratio and in blue the night radiation ratio. The horizontal lines correspond to the threshold to classify a day/night as clear or cloudy. The blue dot placed in day 14th July, 2019 corresponds to the night of 14th-15th July, 2019.

Observing the solar radiation ratio orange bars, most of the days are around 0.7 except for 4 (17th, 26th, 27th July and 7th August). From the experimentation notebook it is known that on 17th and 26th of July it was raining and the sky was completely cloudy during all day. Thus, for the sake of classifying the days in a simple and easy way and without any aim of generalizing this classification outside this paper, a solar radiation threshold of 0.55 is defined, so the days with higher ratio are considered clear and the days below this ratio cloudy.

Looking at the IR radiation blue dots, it is observed that they present lower oscillation than solar irradiation ratios. Note that the two highest values of radiation ratio nights are associated to days with very low solar radiation ratios (cloudy days). Assuming that it is reasonable that the night previous to a cloudy day has been a cloudy night as well, and knowing by theory that high humidity and high cloud cover is associated to higher sky IR radiation values and lower radiative cooling potential, it is taken the lowest IR radiation ratio corresponding to the previous night of cloudy day (26th - 27th July) as reference value to classify in a binary way the night cloudiness. This value corresponds to 0.78. Again, this classification is specific to this experimentation and should not be applied in other contexts.

Therefore, from all the monitoring period, the cloudy days were 17th, 26th, 27th July and 7th August, 2019; and the cloudy nights were 16th, 25th, 26th July and from 6th to 11th August. The rest of the monitoring period was considered clear days and nights.

From Figure 6 to Figure 9 the average daily values of the RCE power, using the eq. 1 previously presented, external temperature and outlet RCE temperature are presented for the four different sky conditions defined above: clear day, cloudy day, clear night and cloudy night along the 5 weeks of experimental testing.

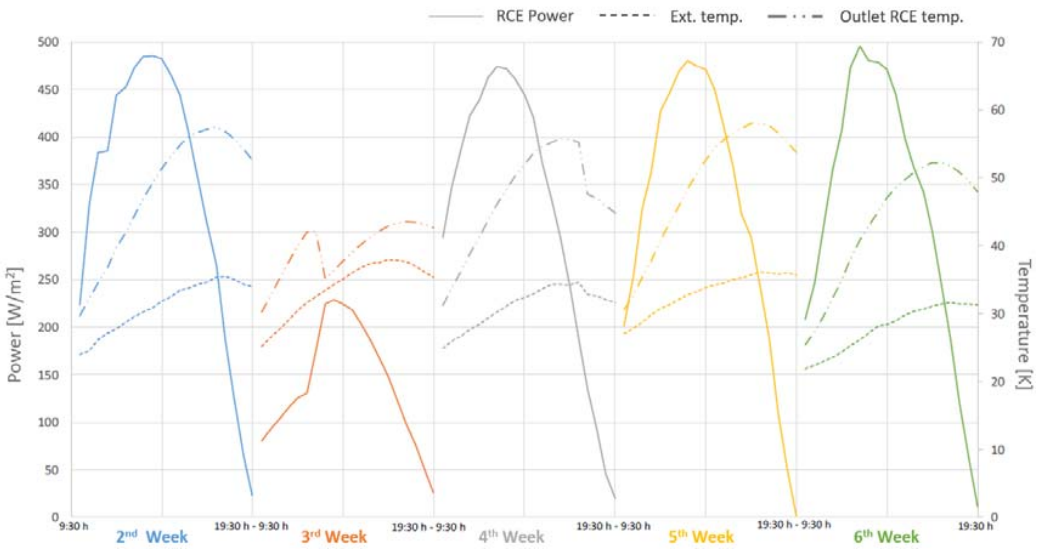

Figure 6: Average clear day corresponding to the experimental week.

In Figure 6, it is observed an average day evolution considering the average values of the clear days corresponding to each experimental week. The first week is not considered as explained in previous sections. During the 3rd week, the RCE was covered during daytime, although the facility was still operating in normal collection mode to prevent overheating. This effect is shown in Figure 6, when the 3rd week results show the lowest RCE power production. Apart from this 3rd week, the behavior of all three parameters presented (RCE power, external temperature and outlet RCE temperature) are almost the same. The continuous line corresponding to the RCE power reaches almost 500 W/m^2 each day, having the highest point during midday, around 1 PM. As expected, water from the RCE keeps increasing its temperature during the day, achieving its maximum of about 56 ºC around 5:30 PM, represented with the dot-dot-dash line. This outlet RCE temperature has the same tendency as the exterior temperature represented with the small dots line.

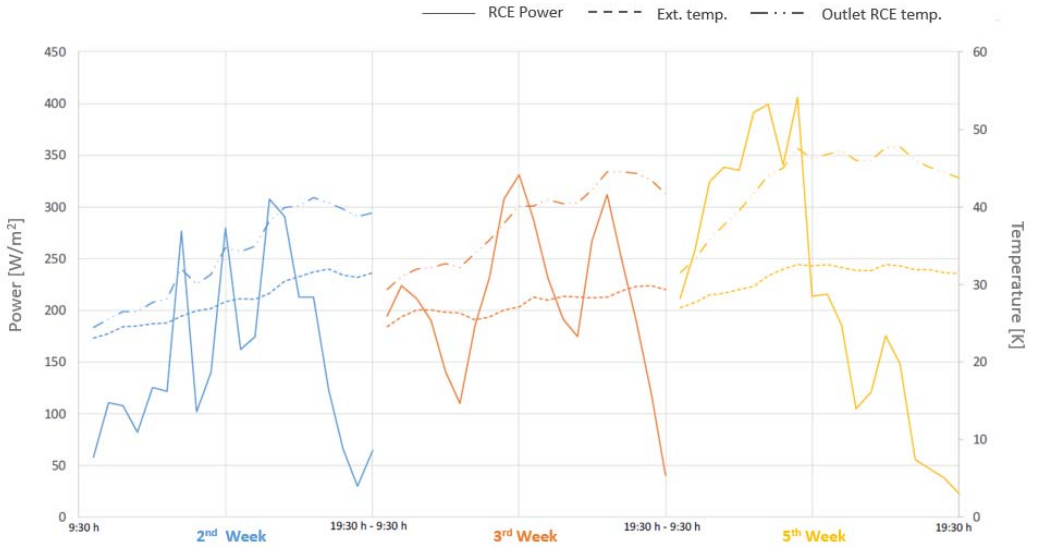

Figure 7: Average cloudy day corresponding to the experimental week.

During the monitoring period and according to our criteria, only four days were considered cloudy. Those days correspond to the 2nd week (17th of July), 3rd week (26th and 27th of July) and 5th week (7th of August). To present the results similar to the clear days, in the above Figure 7 are presented the weeks corresponding to the cloudy days, but in this case there is only one cloudy day for the 2nd and 5th week, and the average of two cloudy days in the 3rd week. In the case of cloudy days the behavior between weeks is also similar, but not as smooth as during clear days. Different RCE power peaks are recorded which might correspond to clear or less cloudy periods of time during the day. As it happened in the clear days, the outlet RCE temperature is increasing during

the day having its maximum between 40-50 ºC around 5:30 PM. In this case the exterior temperature remains quite stable around 30 ºC.

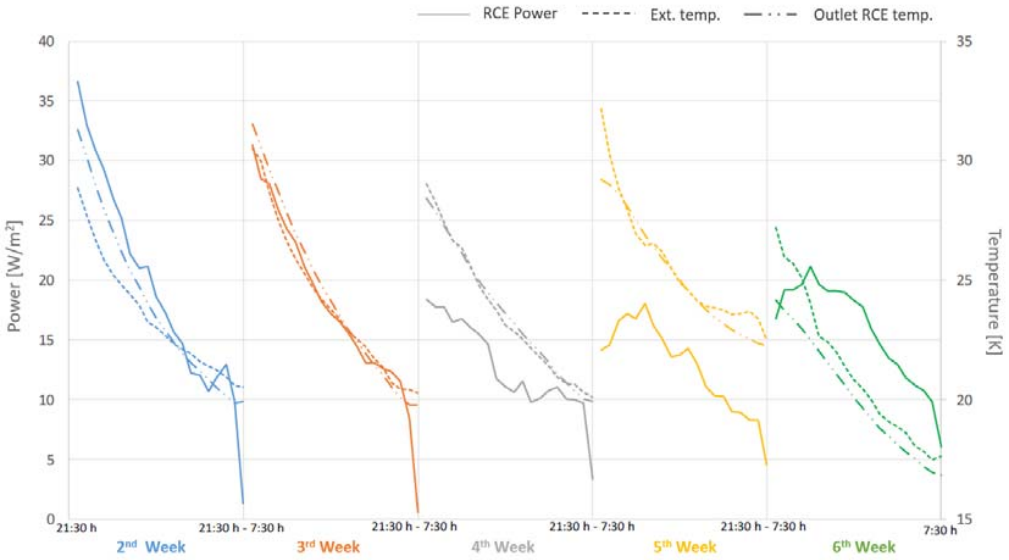

Figure 8: Average clear night corresponding to the experimental week.

In Figure 8 is presented the clear night behavior of a typical night for the five weeks of experimental tests. As it happened during the analysis of clear days, the evolution of the temperatures and the RCE power is similar for all weeks. As the external temperature is decreasing during the night, the RCE power is also decreasing having higher values at the beginning of the night, at 9:30 PM. This RCE power values decrease from 30 - 35 W/m^2 for the 2nd and 3rd weeks, and from 17 – 20 W/m^2 for the 4th, 5th and 6th weeks to 10 W/m^2 before sunrise at 7 AM. From 3:30 AM the outlet temperature of the RCE is lower than the exterior temperature (22 ºC) and it remains below it until the sunrise when the radiative cooling mode is over, except from the 6th week when the outlet RCE temperature is all the time under the external temperature. This subambient cooling temperature goes up to 3ºC below the external temperature. As it is observed in Figure 8, the RCE power decreases during the experimentation period, obtaining lower RCE powers for the 4th and 5th weeks of experiments than the 1st and 2nd weeks. This decreasing power might be caused by the aging and deterioration of the PE film but also due to the dust accumulated on it. Thus, before the last week of experiments, the film was cleaned with an electrostatic towel and an increase of 3 W/m^2 in the RCE power was registered. However, cleaning the polyethylene film was not enough for obtaining the RCE power results of the first weeks of experiments.

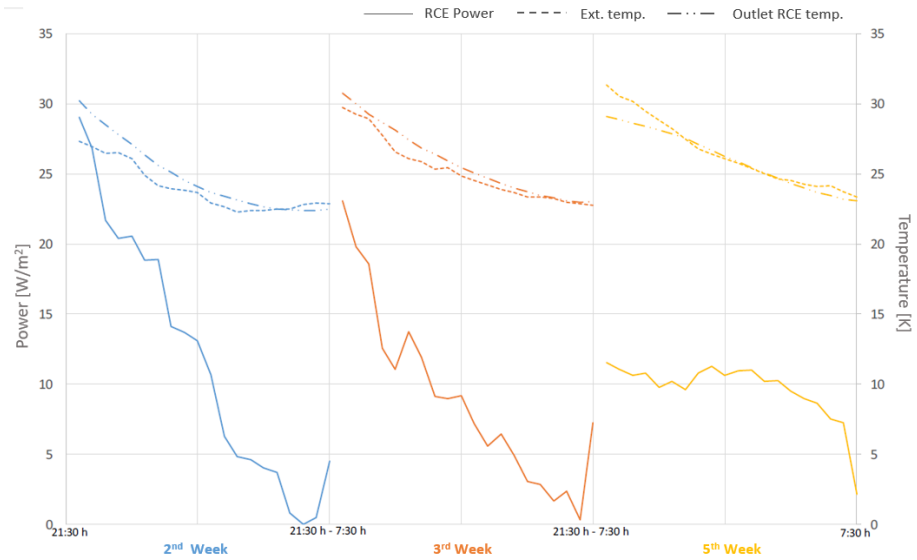

Figure 9: Average cloudy night corresponding to the experimental week.

In the above Figure 9, the average cloudy nights considered following our criteria described before, are presented according to the corresponding week: 16th of July (2nd week), 25th and 26th of July (3rd week) and from 6th to 11th of August (5th week). The behavior of the RCE is almost the same throughout the weeks monitored. As it happened during clear nights, the RCE power is decreasing during the night as the external and the outlet RCE temperature, which are very similar during all the night, are also decreasing. This effect occurs because the radiative cooling power depends on the surface temperature of the absorber, which is decreasing during the night. It has been recorded subambient cooling temperatures for the outlet RCE temperature around 6 AM during 2nd and 3rd week, and a bit before (around 3:30 AM) for the 5th week, as it happened for the clear nights.

Table 1 shows average and maximum values for the temperature difference between the outlet of the RCE and the external temperature and the thermal power obtained depending on the sky condition.

Tab. 1: Average and maximum values for the temperature difference in the RCE and thermal RCE power .

	Solar collection mode		**Radiative cooling mode**	
	Clear day	**Cloudy day**	**Clear night**	**Cloudy night**
Average ΔT (ºC)	16.93	5.86	- 1.1	-0.6
Max. ΔT (ºC)	22.53	9.57	-3.04	-2.21
Average RCE power (W/m^2)	573.69	385.22	-15.57	-9.73
Max. RCE power (W/m^2)	865.27	696.02	-36.60	-29.03

To calculate the average and the maximum temperature difference, it has been considered only the values during the period when a subambient cooling temperature has been registered in the RCE.

The results show similar behavior according to the sky conditions. During clear sky condition, the RCE power obtained is higher for solar radiation and radiative cooling collection. The same happens with the average and maximum subambient cooling temperature, obtaining higher values for clear sky condition.

For clear days the average RCE power is 573.69 W/m^2, having its maximum around midday with a value of 865.27 W/m^2, and the outlet temperature is about 17 ºC higher than the external temperature which rises up to 37 ºC.

During cloudy days the RCE power obtained is much lower, having a maximum value of 696.02 W/m^2 and average of 385.22 W/m^2 The outlet temperature of the RCE is also lower, increasing just an average of 5.86 ºC and a maximum of 9.57 ºC from the external temperature which does not exceed 32 ºC.

Regarding the radiative cooling analysis, comparing the results with the solar collection mode, those are much lower. For clear nights, the maximum RCE power is -36.60 W/m^2, and the average power obtained is -15.57 W/m^2. The outlet RCE temperature is under the ambient temperature an average of -1.1 ºC and a maximum of -3.04 ºC.

For the cloudy nights, when the sky infrared radiation is higher, the results are even lower. The average value of the RCE power on cloudy nights is about 10 W/m^2 with maximum values of 29 W/m^2 for the first two weeks analyzed. The average difference between the outlet RCE temperature and the external temperature is -0.6 ºC, having the maximum difference in the last week of experiments obtaining a difference of -2.21 ºC.

As expected, the results for the collection mode are much higher than the radiative cooling mode. The average thermal RCE power is almost 37 times higher during solar collection mode.

5. Conclusions

The RCE is a possible solution for space conditioning. The concept of combining solar collection and radiative cooling in a single prototype is possible and it produces similar solar collection power with an additional radiative cooling power during night time. During solar collection mode higher power is achieved than during radiative cooling mode. Although radiative cooling may not be, nowadays, the solution for space cooling, it can complement conventional cooling systems, reducing the emissions since it is a renewable energy.

The results from the monitoring period presented in this study demonstrate the potential of the Radiative Cooler and Emitter concept to produce hot water during daytime and cool water below room temperature during night time with a single equipment.

Another result from the experimentation is the negative effect of the dust and dirt accumulation on the cover of the RCE. After the 5th week of experiments, the polyethylene and the glass cover have been thoroughly cleaned and better results are obtained in the last week of experiments, with a significant performance improvement for the radiative cooling mode during clear days, despite the deterioration of the polyethylene film.

More research on the adaptive cover, the use of other materials and the PE aging is needed. With a more resistant material to the weather conditions and better optical characteristics (high transmittance in the atmospheric window) the deterioration observed during this experimentation will not appear or it will take longer, and higher values for the radiative cooling power will be achieved.

6. Acknowledgment

The work was partially funded by the Spanish government under grant agreement RTI2018-097669-AI00 (Ministerio de Ciencia, Innovación y Universidades) and by Fundación Iberdrola España under project "Desarrollo y evaluación de un equipo para producción combinada de frío y calor mediante refrigeración radiante y captación solar". The authors would like to thank Generalitat de Catalunya for the project grant given to their research group (2017 SGR 659). Ariadna Carrobé would like to thank the Secretaria d'Universitats i Recerca del Departament d'Empresa i Coneixement de la Generalitat de Catalunya for its research fellowship. The authors would like to thank Ginesta Jové Artal for her final degree project.

7. References

Bhatia, B., Leroy, A., Shen, Y., Zhao, L., Gianello, M., Li, D., Gu, T., Hu, J., Soljačić, M., Wang, E.N., 2018. Passive directional sub-ambient daytime radiative cooling. Nature Communications 9, 5001. https://doi.org/10.1038/s41467-018-07293-9

European Commission, n.d. Energy efficiency in buildings [WWW Document]. European Commission - European Commission. URL https://ec.europa.eu/info/news/focus-energy-efficiency-buildings-2020-feb-17_en (accessed 7.22.20).

Feng, J., Santamouris, M., Shah, K.W., Ranzi, G., 2019. Thermal analysis in daytime radiative cooling. IOP Conference Series: Materials Science and Engineering 609, 072064. https://doi.org/10.1088/1757-899X/609/7/072064

Kristin, S., Sverrisson, F., Appavou, F., Brown, A., Epp, B., Ledreiter, A., 2016. Renewables 2016 Global Status Report. Paris, France.

Nilsson, T.M.J., Niklasson, G.A., 1995. Radiative cooling during the day: simulations and experiments on pigmented polyethylene cover foils. Solar Energy Materials and Solar Cells 37, 93–118. https://doi.org/10.1016/0927-0248(94)00200-2

Pech-May, N.W., Retsch, M., 2020. Tunable daytime passive radiative cooling based on a broadband angle selective low-pass filter. Nanoscale Adv. 2, 249–255. https://doi.org/10.1039/C9NA00557A

UE 2018/844, 2018. , 156.

Vall, S., Medrano, M., Solé, C., Castell, A., 2020. Combined Radiative Cooling and Solar Thermal Collection: Experimental Proof of Concept. Energies 13, 893. https://doi.org/10.3390/en13040893

Yalçın, R.A., Blandre, E., Joulain, K., Drévillon, J., 2020. Daytime radiative cooling with silica fiber network. Solar Energy Materials and Solar Cells 206, 110320. https://doi.org/10.1016/j.solmat.2019.110320